Soft Matter

Amphiphilic, thixotropic additives for extrusion-based 3D printing of silica-reinforced silicone

Journal:	*Soft Matter*
Manuscript ID	SM-ART-02-2021-000288
Article Type:	Paper
Date Submitted by the Author:	24-Feb-2021
Complete List of Authors:	Suriboot, Jakkrit; Texas A&M University College Station, Biomedical Engineering Marmo, Alec; Texas A&M University College Station, Materials Science and Engineering Ngo, Bryan Khai; Texas A&M University College Station, Biomedical Engineering Nigam, Aman; Texas A&M University College Station, Mechanical Engineering Ortiz-Acosta, Denisse; Los Alamos National Laboratory, Chemistry Division Tai, Bruce; Texas A&M University College Station, Mechanical Engineering Grunlan, Melissa; Texas A&M University College Station, Biomedical Engineering

Journal Name

ARTICLE

Amphiphilic, thixotropic additives for extrusion-based 3D printing of silica-reinforced silicone

Received 00th January 20xx,
Accepted 00th January 20xx

DOI: 10.1039/x0xx00000x

www.rsc.org/

Jakkrit Suriboot,[a] Alec C. Marmo,[b] Bryan Khai D. Ngo,[a] Aman Nigam,[c] Denisse Ortiz-Acosta,[d] Bruce L. Tai,[c] and Melissa A. Grunlan*[a,b,d]

The ability to utilize extrusion-based, direct ink write (DIW) 3D printing to create silica-reinforced silicones with complex structures could expand their utility in industrial and biomedical applications. Sylgard 184, a common Pt-cure silicone, lacks the thixotropic behavior necessary for effective printing and its hydrophobicity renders cured structures susceptible to biofouling. Herein, we evaluated the efficacy of various PEO-silane amphiphiles (PEO-SAs) as thixotropic and surface modifying additives in Sylgard 184. Eight amphiphilic PEO-SAs of varying architecture (e.g. linear, star, and graft), crosslinkability, and PEO content were evaluated. Modified formulations were also prepared with additional amounts of silica filler, both a hexamethyldisilazane (HMDS)-treated and a dimethyldichlorosilane (DiMeDi)-treated types. Numerous PEO-SA modified silicone formulations demonstrated effective water-driven surface hydrophilicity that was generally diminished with the addition of HMDS-treated silica filler. While increased yield stress was observed for PEO-SA modified silicones with added HMDS-treated filler, none achieved the intial target for 3D printing (> 1,000 Pa). Only the formulations containing the DiMeDi-treated filler (17.3 wt%) were able to surpass this value. These formulations were then tested for their thixotropic properties and all surpassed the targets for recovered storage modulus (G') (> 1,000 Pa) and loss factor (< 0.8). In particular, the triblock linear PEO-SA produced exceptionally high recovered G', low loss factor, and substantial water-driven restructuring to form a hydrophilic surface. Combined, these results demonstrate the potential of silicones modified with PEO-SA SMAs for extrusion-based, DIW 3D printing applications.

Introduction

Silicones such as crosslinked polydimethylsiloxane (PDMS) are useful in many applications due to their unique properties, including elastomeric mechanical behavior and oxidative stability.[1-3] To further enhance toughness and strength, silicones are often reinforced with silica fillers.[4] Using conventional fabrication techniques such as compression molding, extrusion, and soft lithography, reinforced silicone objects have been fabricated for applications such as flexible and wearable electronics,[5-7] soft robotics,[8-9] and medical devices (e.g. catheters, and maxillofacial prostheses).[10-12] 3D printing represents an opportunity to fabricate silicone devices with more intricate structures.[13-14] However, thixotropic behavior is required of the "ink" in extrusion-based 3D printing (i.e. direct ink writing, DIW).[15-17] Thixotropy is a time-dependent rheological behavior characterized by fluidification of a material under high shear and stiffening of a material at rest or low shear rates.[18] In this way, a thixotropic silicone ink would be readily extruded through the printing nozzle but also maintain its printed shape. In addition, while beneficial in some applications, the hydrophobicity of silicones can be detrimental in certain biomedical applications, particularly in terms of biofouling.[19] Thus, a thixotropic silicone ink with on-demand hydrophilicity for improved wettability and fouling resistance could broaden their utility.

To achieve a hydrophilic silicone surfaces, a variety of physical and chemical processes have been utilized.[20] Genzer et. al examined the use of oxygen plasma in conjunction with ultraviolet (UV) radiation, creating a hydrophilic silica-like surface.[21] Lin et. al grafted polyamidoamine dendrimers onto the surface after oxygen plasma, reducing the water contact angle from 108.1° to 31.8°.[22] However, both methods are limited because they rely on oxygen plasma that is associated with an increase in the Young's modulus of the surface.[23] de Campos et. al attempted to circumvent the use of oxygen plasma by modifying the surface with PEG-divinyl ether via hydrosilylation.[24] Although they were able to lower the contact angle to 10°, there was hydrophobic recovery to 70° after just two days. Rather than a complex, direct surface modification approach, the simple addition of a bulk additive that subsequently induces hydrophilic surface properties is an attractive alternative.

Previous work in our group has focused on the bulk incorporation of linear poly(ethylene oxide) (PEO)-silane amphiphiles (PEO-SAs) as surface-modifying additives (SMAs) in silicones for water-driven surface hydrophilicity and biofouling resistance.[25-33] The PEO-SAs were comprised of an oligo(dimethyl siloxane) ($ODMS_m$) tether, a PEO segment (PEO_8), and either a triethoxysilane (TES) group [α-$(EtO)_3$-$(CH_2)_2$-$ODMS_m$-*block*-PEO_8-OCH_3; m = 13 or 30] or silane (Si-H) group [H-Si-$ODMS_m$-*block*-PEO_8-OCH_3; m = 13 or 30]. Moreover, the presence of a crosslinkable group did not appear essential to maintaining long-term efficacy, indicating that the ODMS tethers physical anchored the SMA within the silicone matrix.[30, 32]

[a] Department of Biomedical Engineering, Texas A&M University, College Station, TX 77843, USA.
[b] Department of Materials Science and Engineering, Texas A&M University, College Station, TX 77843, USA.
[c] Department of Mechanical Engineering, Texas A&M University, College Station, TX 77843, USA.
[d] Chemistry Division, Los Alamos National Laboratory, Los Alamos, NM 87545, USA.
[e] Department of Chemistry, Texas A&M University, College Station, TX 77843, USA.
*Corresponding Author, E-mail: mgrunlan@tamu.edu, Tel: +1 979 845 2406.

Notably, this enhanced hydrophilicity was not seen for silicones modified with the analogous, non-amphiphilic PEO-silanes (i.e. no ODMS tether; conventional "PEO-silane controls").[25-33] This highlights the importance of the ODMS tether, not only in serving as a physical anchor, but also in increasing the miscibility of the SMA in the silicone network for enhanced water-driven surface-restructuring. Sylgard 184 cures via a Pt-catalyzed hydrosilylation reaction between vinyl groups (base, "Part A") and Si-H groups (curing agent, "Part B"). Thus, this system would allow for crosslinking with the Si-H-terminated PEO-SAs. Recently, we reported that such an amphiphilic PEO-SA SMA was incorporated into Sylgard 184 at varying concentrations to form microfluidic channels produced by molding.[34] However, their rheological properties were not assessed or manipulated towards achieving thixotropic behavior.

In this work, amphiphilic oligomeric additives were explored for their ability to achieve thixotropic behavior and to optionally induce surface hydrophilicity when blended with a common silica-reinforced silicone, Sylgard 184. According to the materials safety data sheet (MSDS), Sylgard 184 "Part A" and "Part B" contains 30-60 wt% and 10-30 wt% dimethylvinylated and trimethylated silica, respectively. Even with these silica fillers, the lack of thixotropy of Sylgard 184, particularly its low yield stress, limits its utility in extrusion-based, DIW 3D printing.[18, 35-38] Generally, the thixotropic behavior of PDMS is increased with silica fillers[39] or carbon nanotube fillers.[40] These additives rely on a combination of their excluded volume and surface-matrix interaction to cause the intended thixotropic properties.[41] Herein, amphiphilic oligomeric additives were added to Sylgard 184, along with additional silica, to synergistically enhance these effects.

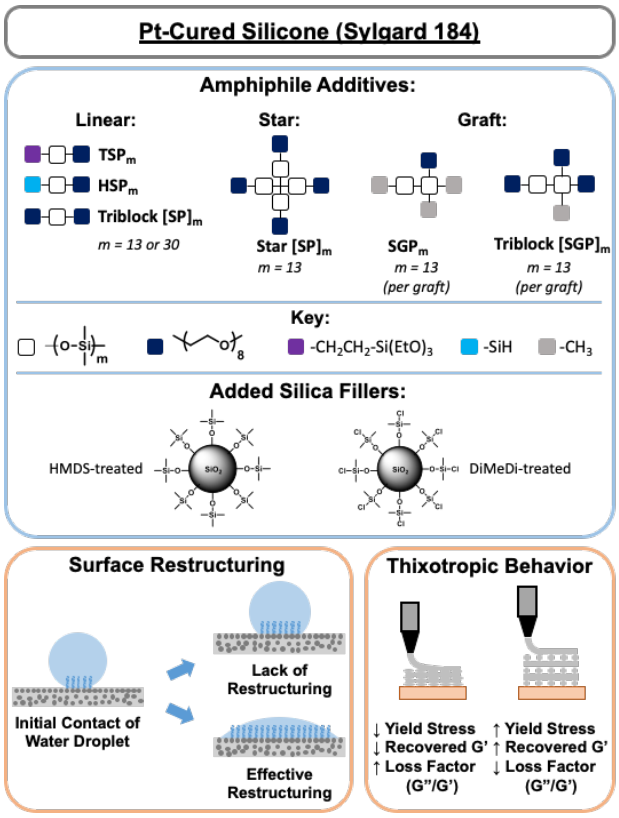

Figure 1. Amphiphilic PEO-SA additives and silica fillers were systematically incorporated into Sylgard 184. The impact on rheological properties and water-driven surface hydrophilicity were systematically evaluated.

Specifically, we sought to investigate Sylgard 184 modified with various PEO-SAs as well as with different added silica fillers (**Figure 1**). The ability of these formulations to achieve water-driven surface hydrophilicity was also examined. Several SMAs were evaluated, with PEO-SAs of varying structural features: **(i)** architecture (e.g. linear, star, graft), **(ii)** crosslinkability with Sylgard 184 matrix (i.e. Si-H-containing ["crosslinkable"] and TES-containing ["non-cross-linkable"]), and **(iii)** PEO content (**Scheme 1, Table S1**). Two types of fillers were utilized: a hydrophobic, hexamethyldisilazane (HMDS)-treated silica filler, and a hydrophilic, dimethyldichlorosilane (DiMeDi)-treated silica filler. We aimed to identify formulations that provided the necessary thixotropic behavior for extrusion-based printing and, optionally, water-driven surface hydrophilicity.

Experimental

Materials

Allyl methyl PEO_8 ("A-PEO_8M") (Polyglykol AM 450; M_n = 292-644 g/mol per manufacturer's specifications; M_n = 424 g/mol per ^{1}H NMR end group analysis, ^{1}H NMR ($CDCl_3$; δ, ppm): 3.35 (s, 3H, OCH_3), 3.51–3.66 (m, 32H, OCH_2CH_2), 4.00 (d, J = 5.4 Hz, 2H, CH_2=$CHCH_2O$), 5.13–5.28 (m, 2H, CH_2=$CHCH_2O$) and 5.82–5.96 (m, 1H, CH_2=$CHCH_2O$)) was kindly provided by Clariant. 1,3,5,7-tetramethylcyclotetrasiloxane (D_4^H), Octamethylcyclotetrasiloxane (D_4), HMDS-treated silica filler (SIS6962.0), hexamethyldisiloxane (HMDSO), tetramethyldisiloxane (TMDS), TES, vinyltriethoxysilane (VTEOS), platinum (Pt)-divinyltetramethyldisiloxane complex (Karstedt's catalyst) in xylene, and α,ω-bis(SiH)$ODMS_{13}$ ($ODMS_{13}$) (M_n = 1000-1100 g/mol per manufacturer's specifications; M_n = 1096 g/mol per ^{1}H NMR end group analysis, ^{1}H NMR ($CDCl_3$; δ, ppm): 0.05–0.10 (m, 78H, $SiCH_3$), 0.19 (d, J = 2.7 Hz, 12H, $OSi[CH_3]_2H$) and 4.67–4.73 (m, 2H, SiH)) were purchased from Gelest. $ODMS_{30}$ (M_n = 2354 g/mol per ^{1}H NMR end group analysis, ^{1}H NMR ($CDCl_3$; δ, ppm): 0.05–0.11 (m, 180H, $SiCH_3$), 0.19 (d, J = 2.7 Hz, 12H, $OSi[CH_3]_2H$) and 4.67–4.73 (m, 2H, SiH)) was prepared as reported via ring opening polymerization of TMDS and D_4.[31] Rhodium (I) tris(triphenylphosphine) chloride (Wilkinson's catalyst), hexamethyldisilazane (HMDS), triflic acid, deuterated chloroform ($CDCl_3$), and solvents were obtained from Sigma-Aldrich. Glass microscope slides (75 × 25 × 1 mm) were purchased from Fisher Scientific. Sylgard 184 was purchased from Dow Corning. Per manufacturer's specifications, the Sylgard 184 base ("Part A") is composed of dimethylvinyl-terminated dimethylsiloxane (> 60 wt%), tetra (trimethylsiloxy) silane (1.0 – 5.0 wt%), and dimethylvinylated as well as trimethylated silica (30 – 60 wt%). The Sylgard 184 curing agent ("Part B") is composed of dimethyl, methylhydrogen siloxane (40 – 70 wt%), dimethylvinyl-terminated dimethylsiloxane (> 15 – 40 wt%), tetramethyl tetravinyl cyclotetrasiloxane (1.0 – 5.0 wt%) and dimethylvinylated as well as trimethylated silica (10 – 30 wt%). DiMeDi-treated silica filler (CAB-O-SIL TS610) was obtained from Cabot Corporation. A commercial thixotropic agent for addition cure silicone elastomers, Quantum Thixo Agent AC, was purchased from Quantum Silicones.

General synthetic approach

All reactions were run under nitrogen with a Teflon-covered stir bar. Chemical structures of synthetic products (**Scheme 1**) were confirmed via ^{1}H NMR spectroscopy using an Inova 500 MHz

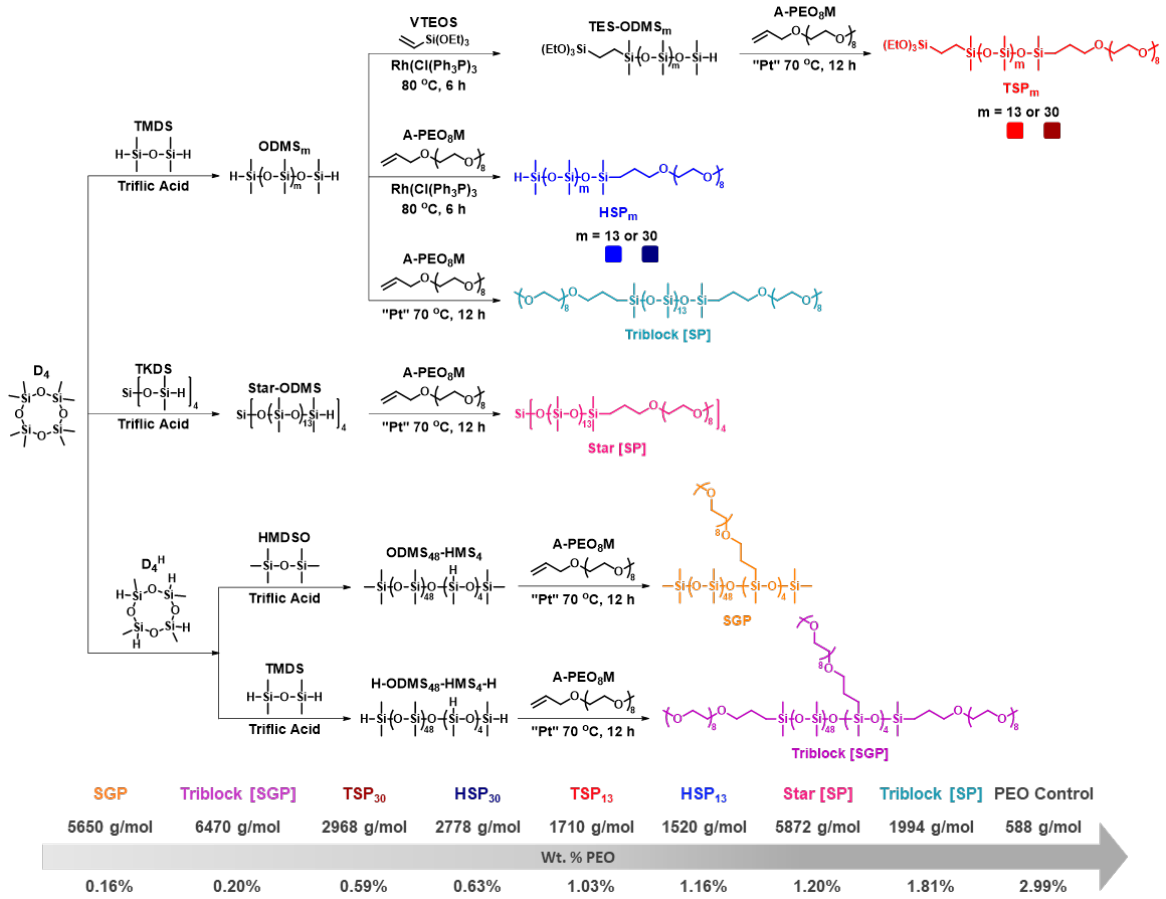

Scheme 1. Synthesis of PEO-silane amphiphile surface-modifying additives (PEO-SA SMAs). **TSP$_m$** (triethoxysilane terminated oligo(dimethylsiloxane)-*b*-PEO); **HSP$_m$** (hydride terminated oligo(dimethylsiloxane)-*b*-PEO); **Triblock [SP]** (PEO-*b*-oligo(dimethylsiloxane)-*b*-PEO); **Star [SP]** (star, oligo(dimethylsiloxane)-*b*-PEO); **SGP** (oligo(dimethylsiloxane)-*b*-oligo(methylsiloxane-*g*-PEO) and **Triblock [SGP]** (PEO-*b*-oligo(dimethylsiloxane)-*b*-oligo(methylsiloxane-*g*-PEO)-*b*-PEO). Molecular weight and wt. % PEO were calculated based on complete conversion of the hydrosilylation reaction and additive structures confirmed by NMR (Figures S3-S10).

spectrometer operating in the Fourier transform mode and with $CDCl_3$ as the standard.

Synthesis of non-amphiphilic "PEO-silane" control. The PEO-silane control [α-$(EtO)_3$-$(CH_2)_3$-PEO_8-OCH_3] was prepared as previously reported using a one-step hydrosilylation protocol.[25] Briefly, TES (Si-H-terminated) was reacted with A-PEO_8M (1:1 molar ratio) via a Karstedt's-catalyzed hydrosilylation reaction. The purified product was clear, colorless, and the ^{1}H NMR was in agreement with that previously reported.[25]

Synthesis of amphiphile precursors:

Star-ODMS, H-ODMS-HMS-H, and ODMS-HMS were prepared using triflic acid-catalyzed ring-opening polymerizations of a cyclic monomer in the presence of suitable end-capping agents, TKDS, TMDS, and HMDSO, respectively. Reagents were combined in sealed round bottom flasks (RBF), and 40 µL of triflic acid was added. Each mixture was stirred at room temperature (RT) for 12 h, and was neutralized with the addition of 94 µL of HMDS (RT, 1 h). The products were purified by filtration through ashless filter paper and yielded colorless liquids.

Synthesis of *Star*-ODMS. D_4 (25 g, 84.29 mmol), TKDS (2.13 g, 6.48 mmol), and triflic acid were reacted to yield the product (23.09 g, 83%). ^{1}H NMR ($CDCl_3$; *δ*, ppm): 0.02-0.13 (m, 336H, SiC*H*$_3$), 4.65-4.70 (m, 4H, Si*H*).

Synthesis of H-ODMS$_{48}$-HMS$_4$-H. D_4 (25 g, 84.29 mmol), D_4^H (1.69 g, 7.02 mmol), TMDS (0.94 g, 7.02 mmol), and triflic acid were reacted to yield the product (23.12 g, 84%). ^{1}H NMR ($CDCl_3$; *δ*, ppm): 0.03-0.26 (m, 312H, SiC*H*$_3$), 4.64-4.71 (m, 6H, Si*H*).

Synthesis of ODMS$_{48}$-HMS$_4$. D_4 (25 g, 84.29 mmol), D_4^H (1.69 g, 7.02 mmol), HMDSO (1.14 g, 7.02 mmol), and triflic acid were reacted to yield the product (22.80 g, 82%). ^{1}H NMR ($CDCl_3$; *δ*, ppm): 0.02-0.20 (m, 318H, SiC*H*$_3$), 4.70 (s, 4H, Si*H*).

Synthesis of amphiphiles with linear architecture:

Synthesis of non-crosslinkable, diblock: TSP$_m$ (m = 13 and m = 30). TSP$_m$ (TES-terminated) was synthesized as previously reported using a two-step hydrosilylation protocol.[25] Briefly, each ODMS$_m$ (m = 13 or 30) underwent a Wilkinson's-catalyzed regioselective hydrosilylation with VTEOS (1:1 molar ratio) to form TES-ODMS$_m$. Next, each product was reacted with A-PEO_8M (1:1 molar ratio) via a Karstedt's-catalyzed hydrosilylation reaction. Purified products were clear, colorless, and ^{1}H NMR was in agreement with that previously reported (Figures S3-S4).[25]

Synthesis of crosslinkable, diblock: HSP_m (m = 13 and m = 30). HSP_m (Si-H-terminated) was synthesized as previously reported using a one-step hydrosilylation protocol.[30] Briefly, each $ODMS_m$ (m = 13 or 30) tether underwent a Wilkinson's-catalyzed regioselective hydrosilylation with A-PEO_8M (1:1 molar ratio). Purified products were clear, colorless, and ^{1}H NMR was in agreement with that previously reported (Figures S5-S6).[30]

Synthesis of non-crosslinkable, triblock: Triblock [SP]. Triblock [SP] was synthesized as previously reported using a one-step hydrosilylation protocol.[30] Briefly, the $ODMS_{13}$ tether underwent Karstedt's-catalyzed hydrosilylation with A-PEO_8M (1:2 molar ratio). The purified product was clear, colorless, and ^{1}H NMR was in agreement with that previously reported (Figure S7).[30]

Synthesis of amphiphiles with star and graft architectures:

Star [SP], SGP and Triblock [SGP] amphiphiles were prepared as follows. A designated amphiphile precursor and A-PEO_8M were dissolved in toluene (20 mL) in a sealed RBF with Karstedt's catalyst (50 µL) and heated to 80 °C. After 12 h, the catalyst was removed from the reaction mixture by adding activated charcoal and heating at 90 ˚C for 2 h. The mixture was cooled to RT and filtered to remove the charcoal. After filtration, the volatiles were removed under reduced pressure and yielded a colorless liquid.

Synthesis of Star [SP]. A-PEO_8M (2.18 g, 5.15 mmol), *star*-ODMS (5.0 g, 1.29 mmol), and Karstedt's catalyst were reacted to yield the product (5.12 g, 71%). ^{1}H NMR ($CDCl_3$; δ, ppm): 0.02-0.13 (m, 336H, $SiCH_3$), 0.48-0.54 (m, 8H, $SiCH_2CH_2CH_2$), 1.54-1.64 (m, 8H, $SiCH_2CH_2CH_2$), 3.37 (s, 12H, OCH_3), 3.41 (t, J = 7.12 Hz, 8H, $SiCH_2CH_2CH_2$), 3.53-3.70 (m, 128H, CH_2CH_2O) (Figure S8).

Synthesis of SGP. AM-PEO_8M (2.15 g, 5.08 mmol), $ODMS_{48}$-HMS_4 (5 g, 1.27 mmol), and Karstedt's catalyst were reacted to yield the product (5.45 g, 76%). ^{1}H NMR ($CDCl_3$; δ, ppm): 0.02-0.18 (m, 318H, $SiCH_3$), 0.45-0.54 (m, 8H, $SiCH_2CH_2CH_2$), 1.57-1.72 (m, 8H, $SiCH_2CH_2CH_2$), 3.40 (s, 12H, OCH_3), 3.42 (t, J = 7.08 Hz, 8H, $SiCH_2CH_2CH_2$), 3.55-3.69 (m, 128H, CH_2CH_2O) (Figure S9).

Synthesis of Triblock [SGP]. A-PEO_8M (3.24 g, 7.64 mmol), H-$ODMS_{48}$-HMS_4-H (5 g, 1.27 mmol), and Karstedt's catalyst were reacted to yield the product (6.12g, 74%). ^{1}H NMR ($CDCl_3$; δ, ppm): 0.03-0.26 (m, 312H, $SiCH_3$), 0.41-0.54 (m, 12H, $SiCH_2CH_2CH_2$), 1.51-1.66 (m, 12H, $SiCH_2CH_2CH_2$), 3.37 (s, 18H, OCH_3), 3.40 (t, J = 7.12 Hz, 12H, $SiCH_2CH_2CH_2$), 3.50-3.70 (m, 192H, CH_2CH_2O) (Figure S10).

Preparation of uncured Sylgard 184 formulations:

Preparation of uncured, unmodified Sylgard 184. Uncured, unmodified Sylgard 184 was prepared by combining 1.7 g of Sylgard 184 "Part A" and 0.17 g of Sylgard 184 "Part B" into a 5 mL FlackTek mixing cup, followed by subjecting to 3000 rpm for 2 min in a FlackTek speedmixer (Model #: DAC 150.1 FVZ-K).

Preparation of uncured "PEO-silane-modified" Sylgard 184. Uncured, silicone modified with the conventional PEO-silane control was prepared by combining 1.7 g of Sylgard 184 "Part A", 5 wt% additive, and additional filler into a 5 mL FlackTek mixing cup. This was mixed via a FlackTek speedmixer at 3000 rpm for 2 min and repeated, as necessary. The mixture was allowed to sit overnight at RT, before 0.17 g of Sylgard 184 "Part B" was added and mixed via speedmixer at 3000 rpm for 2 min.

Preparation of uncured "PEO-SA-modified" Sylgard 184. Uncured, silicone modified with a PEO-SA was prepared by combining 1.7 g of Sylgard 184 "Part A", 5 wt% SMA, and any additional silica filler into a 5 mL FlackTek mixing cup. This was mixed via a FlackTek speedmixer at 3000 rpm for 2 min and repeated, as necessary. The mixture was allowed to sit overnight at RT, before 0.17 g of Sylgard 184 "Part B" was added and mixed via speedmixer at 3000 rpm for 2 min.

Preparation of uncured "Thixo Agent AC-modified" Sylgard 184. Uncured, silicone modified with the commercial thixotropic agent was prepared by combining 1.7 g of Sylgard 184 "Part A", 17.3 wt% Thixo Agent AC, and any additional silica filler into a 5 mL FlackTek mixing cup. This was mixed via a FlackTek speedmixer at 3000 rpm for 2 min and repeated, as necessary. The mixture was allowed to sit overnight at RT, before 0.17 g of Sylgard 184 "Part B" was added and mixed via speedmixer at 3000 rpm for 2 min.

Incorporation of Silica Filler. HMDS-treated and DiMeDi-treated silica filler were each incorporated into selected aforementioned modified Sylgard 184 formulations (5 or 17.3 wt%) with the speedmixer at 3000 rpm for 2 min.

Fabrication of Sylgard 184 films:

Preparation of bulk-modified Sylgard 184 films. Glass microscope slides were sequentially rinsed with dichloromethane and acetone, followed by drying in a 120 °C oven overnight. Polyisobutylene rubber was cut into a square shape (44 x 44 x 1 mm) with a square hole in the middle (30 x 30 x 1 mm). This construct was placed on the glass slide and sealed on each edge with binder clips. These were preheated to 60 °C and the previously prepared Sylgard 184 mixtures (i.e. "uncured") were poured into the mold and placed in a vacuum oven. The vacuum was set to 60 ˚C and pulled at 30 mmHg for 10 – 15 min to degas the films. Next, the vacuum was released and the films were allowed to cure for 2 h at 90 °C. Film thickness (via electronic callipers) was 0.17 ± 0.02 mm.

Methods

Static Water Contact Angle (θ_{static}). Water-driven surface restructuring of silicone films were characterized with θ_{static} measurements using a CAM-200 goniometer (KSV instruments) equipped with an automatic dispenser, video camera, and drop-shape analysis software (Attention Theta). Immediately after fabrication, a 5 µL deionized water droplet was placed on the film and θ_{static} was iteratively measured over a 2 min period in 15 s intervals. The reported θ_{static} values are an average and standard deviation of three measurements made on different regions of the sample film.

Yield Stress. Measurements were recorded on an AntonParr Physica MCR 301 (gap: 1000 µm, measuring cone: 10 mm, sample: ~ 0.5 g). Shear rate was held constant (10 Hz) during an oscillatory amplitude sweep (3 - 3000 Pa), with yield stress determined when G'/G" = 2. The reported yield stress values are an average and standard deviation of three measurements taken from a single batch of uncured silicone.

3 Interval Thixotropy Test (3ITT). Measurements were recorded on an AntonParr Physica MCR 301 (gap: 1000 µm; measuring cone: 10 mm; sample: ~ 0.5 g). The following sequence of steps was performed: (1) 120 s of oscillation at a constant 1% strain amplitude, (2) 120 s of rotation at a constant shear rate of 1,000 Hz, (3) 300 s of oscillation at a constant 1% strain amplitude (i.e. the recovery period). Reported values of recovered storage modulus (G') and loss factor (G"/G') were taken from the end of the 300 s recovery period. The reported line graph values are an average of three measurements taken from the same batch of uncured silicone. The storage modulus and loss factor values are an average and standard deviation of three measurements taken from a single batch of uncured silicone (Figure S1).

3D Printing. An extrusion-based 3D printer using a pneumatic material dispenser was developed for evaluating the printability of the uncured silicone formulations (Figure S2). A given uncured silicone formulation was loaded into a 30-mL syringe and was pressurized up to 551 kPa (80 psi) to control the dispensing rate. The extrusion outlet was 4 mm wide in order to accommodate the highest pressure available for this system. Then, the syringe was attached to a commercial 3D printer to enable programmed motion of printing. In this experiment two prints were made: (1) spooling into a layered coil, and (2) two layers of a grid pattern with 20 mm spacing.

Results and discussion

Characterization of modified Sylgard 184

The ability of modified Sylgard 184 films to undergo water-driven surface restructuring to form a PEO-enriched surface was examined via contact angle analysis. Amphiphilic PEO-SAs and the PEO-silane control were each introduced at 5 wt% along with varying amounts of additional silica filler. Additionally, the yield stresses and thixotropic properties of the uncured silicone mixtures were assessed to determine feasibility in extrusion-based 3D printing.

Contact angle analysis. We previously used AFM to verify the water-driven formation of a PEO-enriched surface of silicone bulk-modified with TSP_{13}.[27] This surface restructuring was accompanied by a reduction in θ_{static} (of a water droplet) over time. Likewise, temporal contact angle measurements taken and θ_{static} values at t = 0 min ($\theta_{static,\ 0\ min}$) and t = 2 min ($\theta_{static,\ 2\ min}$) were used to assess a modified silicone's ability to undergo water-driven surface restructuring to rapidly yield a hydrophilic surface. Initially, this was evaluated when Sylgard 184 was modified with selected amphiphilic PEO-SAs (5 wt%) (of varying architectures as well as crosslinkability) and the PEO-control (5 wt%), all without additional filler (**Figure 2a, Table S2**). As expected, the unmodified silicone was hydrophobic ($\theta_{static,\ 2\ min}$ > 90°) with minimal restructuring (i.e. negligible decrease in $\theta_{static,\ 2\ min}$ versus $\theta_{static,\ 0\ min}$). When modified with the PEO-silane control, the silicone was similarly hydrophobic due to limited surface restructuring ($\theta_{static,\ 2\ min}$ > 90°), consistent with our previous studies.[25-33] Since this additive contained the highest PEO content (~ 3.0 wt%), it emphasizes the necessity of the ODMS tether for effective restructuring of the SMA. In contrast, silicones modified with the amphiphilic PEO-SAs underwent rapid and substantial water-driven surface restructuring. While most were initially hydrophobic ($\theta_{static,\ 0\ min}$ > 90°), surfaces were characterized by varying extents of decreases in $\theta_{static,\ 2\ min}$ and resulting surface hydrophilicity that largely correlated with PEO content of the additive. $\theta_{static,\ 2\ min}$ increased in the order: Triblock [SP] (~ 11°) < Star [SP] (~ 14°) < TSP_{13} (~ 33°) < HSP_{13} (~ 46°) < HSP_{30} (~ 59°) ≈ TSP_{30} (~ 62°) < SGP (~ 80°) ≈ Triblock [SGP] (~ 82°). Of these, Triblock [SP] contains the highest PEO content (~ 1.8 wt%) versus the other amphiphilic additives. The silicone modified with Triblock [SP] underwent extensive water-driven surface restructuring almost immediately after the droplet contacted the silicone surface ($\theta_{static,\ 0\ min}$ ~ 31°), becoming even more hydrophilic after just 2 min ($\theta_{static,\ 2\ min}$ ~ 11°). The silicone modified with Star [SP], having the next highest PEO content (~1.2 wt%), also produced a modified silicone that exhibited extensive restructuring. The other linear PEO-SAs were effective but to lesser extents. Even with similar PEO contents (~ 1.1 wt%, average value), silicones modified with TSP_{13} and HSP_{13} did not restructure as extensively as with Star [SP] or Triblock [SP]. The graft PEO-SAs (i.e. SGP and Triblock [SGP]) both produced modified silicones with relatively minimal surface restructuring, possibly due to their low PEO contents (~ 0.16 and 0.20 wt%).

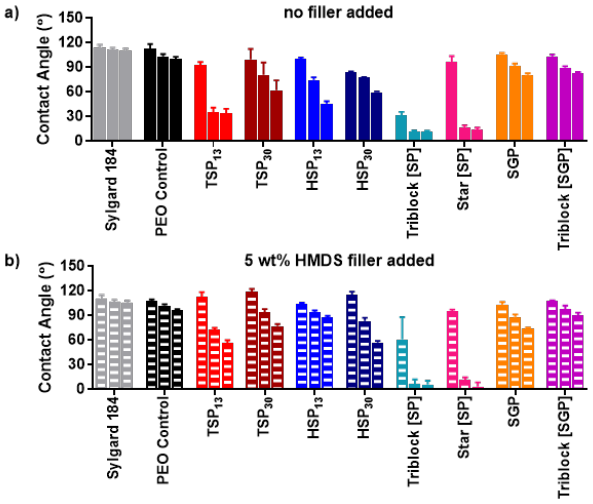

Figure 2. Contact angle at 0, 1, and 2 min of (a) silicone films prepared with 5 wt% of the PEO-silane control or with 5 wt% of amphiphilic PEO-SAs; no additional filler added and (b) analogous silicone films prepared with 5 wt% additional HMDS-treated silica filler.

Next, an analogous series of silicones were prepared but with 5 wt% HMDS-treated filler added (**Figure 2b, Table S3**). Overall, the trend in relative hydrophilicity was maintained as for the aforementioned formulations; with added filler, $\theta_{static,\ 2\ min}$ increased in the order: Star [SP] (~ 3°) < Triblock [SP] (~ 5°) < TSP_{13} (~ 56°) < HSP_{30} (~ 57°) < SGP (~ 74°) < TSP_{30} (~ 77°) < HSP_{13} (~ 87°) < Triblock [SGP] (~ 90°). Thus, when the silicone was modified with Triblock [SP] and Star [SP], it continued to exhibit significant hydrophilicity while those modified with Triblock [SGP] were the most hydrophobic. Intermediate hydrophilicities were achieved with TSP_{13}, HSP_{30}, SGP and TSP_{30}, but the additional filler substantially diminished hydrophilicity. In contrast, the silicone was modified with Triblock [SP] or Star [SP] were actually more hydrophilic versus those prepared without additional filler. Again, despite its high PEO content (~3 wt%), the silicone modified with the PEO-silane control remained hydrophobic.

Yield stress of uncured silicone formulations. The ability of uncured silicone to maintain its printed shape is critical in extrusion-based 3D printing. The value of yield stress depicts the minimum stress required for the fluid to deform. Therefore, yield stress is a useful factor to predict the 3D printability of a given formulation. For

extrusion-based, DIW 3D printing, a yield stress of 1,000 Pa is considered a necessary minimum value.[42] Select PEO-SAs were chosen on the basis of their ability, or lack thereof, to induce a hydrophilic surface. Those with intermediate restructuring, such as $TSP_{13/30}$ and $HSP_{13/30}$, were not included. The PEO-silane control was also not included in further testing as it did not produce a measurable yield stress even after the addition of various fillers.

Initially, we evaluated the yield stress of Sylgard 184 modified with the selected amphiphilic PEO-SAs, without any added filler (**Figure 3a, Table S4**). The unmodified silicone did not produce a measurable yield stress value. In contrast, modification with the PEO-SAs resulted in significantly improved yield stress values, increasing in the order: Triblock [SGP] (40 Pa) = SGP (40 Pa) < Star [SP] (75 Pa) < Triblock [SP] (141 Pa). The same formulations were also prepared with the addition of 5 wt% HMDS-treated silica filler (**Figure 3b, Table S4**). The unmodified silicone still did not produce a measurable yield stress value. For PEO-SA modified formulations, yield stress values did not improve substantially, and unexpectedly decreased in most cases, increasing in the order: Triblock [SGP] (22 Pa) < SGP (31 Pa) < Star [SP] (65 Pa) < Triblock [SP] (87 Pa). Thus, none attained the yield stress target of 1,000 Pa. To further probe its potential to enhance yield stress, the amount of the hydrophobic HMDS-treated silica filler was increased to 17.3 wt% (**Figure 3c, Table S4**). Yield stress increased in the order: Triblock [SP] (84 Pa) < Triblock [SGP] (92 Pa) < Star [SP] (194 Pa) < SGP (212 Pa). Still, while higher amounts of this filler increased the yield stress of all formulations, none were able to reach the aforementioned target.

Next, the same formulations were prepared with the addition of a more hydrophilic, DiMeDi-treated silica filler at 17.3 wt% (**Figure 4, Table S5**). Compared to the HMDS-treated silica, the effect of the DiMeDi silica on sample yield stress was remarkable. With the added silica, the unmodified silicone showed a significant increase in yield stress to 539 Pa. For silicone modified with PEO-SAs, all formulations exceeded the target yield stress, increasing in the order: Triblock [SGP] (1,307 Pa) < Star [SP] (1,405 Pa) < SGP (1,727 Pa) < Triblock [SP] (3,385 Pa). Thus, the interaction between the DiMeDi silica filler and the PEO-SAs was successful in being able to increase yield stress.

Thixotropic behavior of uncured silicone formulations. For a material to be a useful DIW 3D printing ink, it must exhibit rapid recovery of the storage modulus (G') after the removal of shear force (i.e. G' > loss modulus, G"). Additionally, the recovered G' must be high enough to be able to support the load of subsequently printed layers and the loss factor (G"/G') must be low enough to avoid slumping. A recovered G' > 1000 Pa, and loss factor < 0.8 have been shown to be minimum values required for successful prints.[43] Thus,

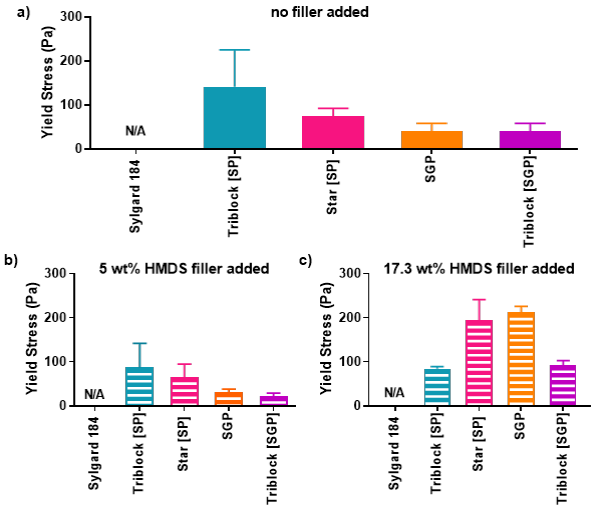

Figure 3. Yield stress of **(a)** uncured modified silicone formulations prepared without additional added filler, **(b)** uncured modified silicone formulations prepared with 5 wt% added HMDS-treated silica filler, and **(c)** uncured modified silicone formulations prepared with 17.3 wt% HMDS-treated silica filler.

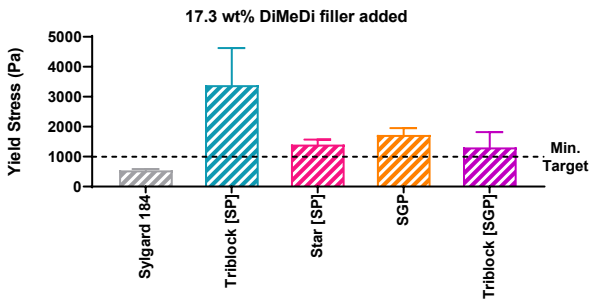

Figure 4. Yield stress of uncured formulations: unmodified silicone (Sylgard 184) and modified silicones, each containing 17.3 wt% additional DiMeDi silica filler, along with the designated additive.

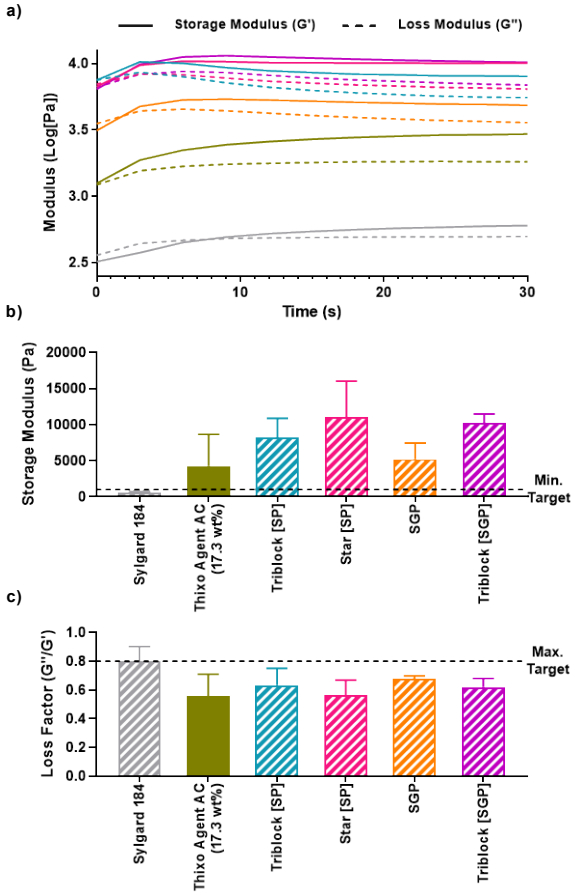

Figure 5. Thixotropic response of uncured formulations: unmodified silicone (Sylgard 184) and modified silicones, each containing 17.3 wt% additional DiMeDi silica filler, along with the designated additive. **(a)** Storage modulus (G') and loss modulus (G") during first 30 sec of recovery period of 3 interval thixotropy test (3ITT); **(b)** G' following the recovery period; **(c)** loss factor (G"/G') following the recovery period.

in addition to determining yield stress, thixotropic behavior of silicone formulations was evaluated using a 3 interval thixotropy test (3ITT) to examine recovery of G' and G" (**Figure S1**). Sylgard 184, modified with 17.3 wt% DiMeDi-treated silica filler and certain PEO-SA addtivies, was evaluated as they were the only formulation to reach the initial benchmark of 1,000 Pa yield stress. An additional formulation modified with 17.3 wt% Thixo Agent AC (also with 17.3 wt% DiMeDi filler) was included. Within 30 seconds of the recovery period, G' and G" had plateaued (**Figure 5a**). All formulations, except the Sylgard 184 (G' = 608.4) achieved the minimum recovered G' (> 1,000 Pa) (**Figure 5b**, **Table S6**). G' increased in the order: Thixo Agent AC (4,272 Pa) < SGP (5,225 Pa) < Triblock [SP] (8,286 Pa) < Triblock [SGP] (10,248 Pa) < Star [SP] (11,023 Pa). In terms of achieving the targeted loss factor (<0.8), the Sylgard 184 was unable to do so **(Figure 5c, Table S7**). However, the modified silicones achieved this target, with loss factor decreasing in the order: SGP (0.68) > Triblock [SP] (0.63) > Triblock [SGP] (0.62) > Star [SP] (0.56) > Thixo Agent AC (0.55).

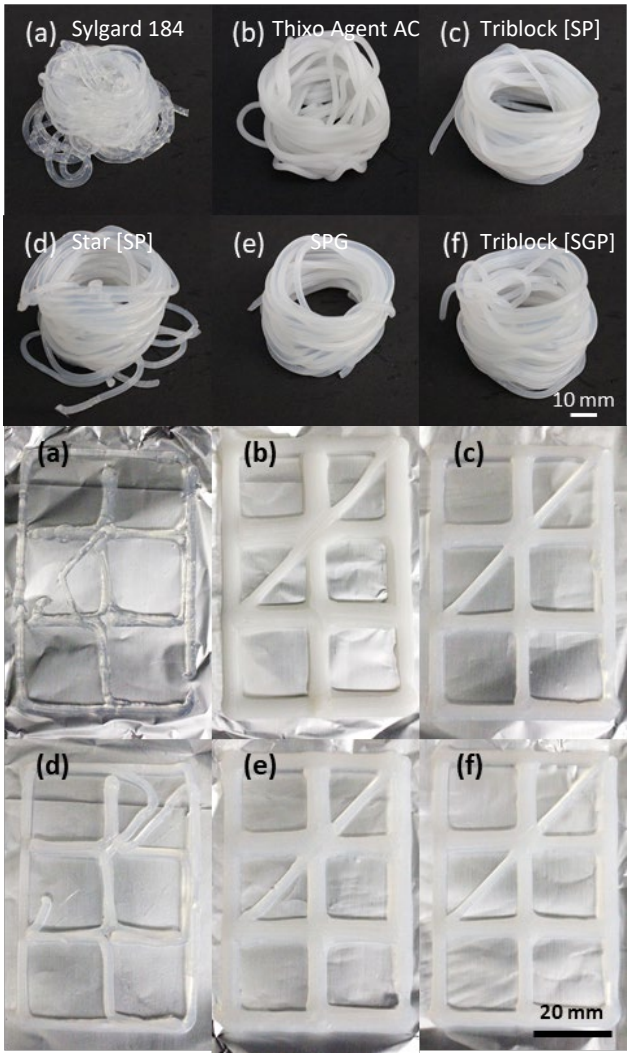

Figure 6. Proof-of-concept extrusion printing of unmodified silicone (Sylgard 184) and modified silicones, each containing 17.3 wt% additional DiMeDi silica filler, along with designated additive. **Top**: Material was allowed to spool out of nozzle into a layered coil. **Bottom**: Two layers of a grid pattern with 20 mm spacing were printed via programmed motion. **(a)** Unmodified Sylgard 184, **(b)** Thixo Agent AC, **(c)** Triblock [SP], **(d)** Star [SP], **(e)** SGP, **(f)** Triblock [SGP].

Printability of silicone formulations. The printability of the formulations used in the 3ITT analyses was assessed with two proof-of-concept prints (**Figure 6**, **Table S9**). A spooled coil was qualitatively assessed for its ability to hold its own shape while a grid pattern was evaluated for line resolution. The Sylgard 184 formulation passed neither of these targets. Interestingly, the Thixo Agent AC formulation, having the lowest loss factor but also a low recovered G', showed some ability to hold its own weight when spooled, but lines lacked resolution. Triblock [SP], Triblock [SGP], and Star [SP] formulation all had high G' recoveries (particularly, Star [SP]) and low loss factors. These all showed stable spooled prints and high-resolution lines. Thus, these PEO-SAs, particularly Star [SP], synergistically interacted with the hydrophilic DiMeDi silica filler to give rise to the desired thixotropic behavior.

Surface hydrophilicity evaluation. In some cases, it is desirable for 3D printed silicone structures to undergo water-driven surface-restructuring whereas in other cases, it is undesirable. Because of their rapid recovery, high recovered G', low loss factor, and previously noted tendency to induce surface hydrophilicity in other formations (i.e. with 5 wt% added HMDS-treated silica filler; **Figure 2**), we investigated this behavior for Sylgard 184 modified with 17.3 wt% DiMeDi filler and 5 wt% Star [SP] or Triblock [SP] PEO-SAs (**Figure 7, Table S9**). As expected, the Sylgard 184 formulation remained hydrophobic ($\theta_{static,\ 2\ min}$ and $\theta_{static,\ 5\ min} \sim 112°$ and 107°, respectively). When modified with Star [SP], restructuring was minimal and resulted in a lack of appreciable hydrophilicity ($\theta_{static,\ 2\ min}$ and $\theta_{static,\ 5\ min} \sim 105°$ and 78°, respectively) and moreover was greatly reduced versus that observed previously ($\theta_{static,\ 2\ min} \sim 3°$; **Figure 2**). Uniquely, the Triblock [SP]-modified silicone formulation exhibited appreciable restructuring and hydrophilicity ($\theta_{static,\ 2\ min}$ and $\theta_{static,\ 5\ min} \sim 61°$ and 44°, respectively), while still reduced from that observed in the other formulation ($\theta_{static,\ 2\ min} \sim 5°$; **Figure 2**).

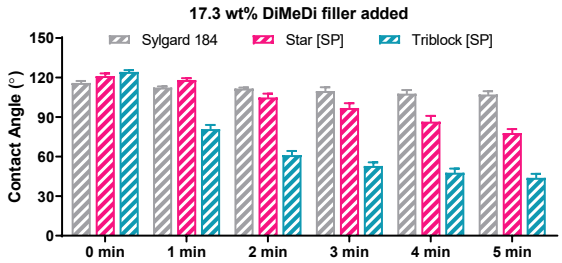

Figure 7. Contact angle at 0, 1, 2, 3, 4, and 5 min (bars, left to right) of silicone films prepared with unmodified silicone (Sylgard 184) and modified silicones, each containing 17.3 wt% additional DiMeDi silica filler, along with 5 wt% of Star [SP] or Triblock [SP].

Conclusions

Herein, the utility of various PEO-silane amphiphiles (PEO-SAs) to induce thixotropic behavior to Sylgard 184, towards improving their utility in extrusion-based 3D printing, was systematically evaluated. The potential to also produce water-driven surface hydrophilicity was also evaluated as resistance to biofouling would be predicted to improve and desirable for some applications. The eight PEO-SAs varied in terms of architecture, crosslinkability with the Sylgard matrix and PEO content. Non-crosslinkable Star [SP] ("star", 1.20 wt% PEO) and Triblock [SP] ("triblock", 1.81 wt% PEO), having the highest PEO wt% content of all PEO-SAs, produced very hydrophilic surfaces when added at 5 wt% to Sylgard 184, even with added HMDS-treated silica (5 wt%). However, the targeted yield stress of

1000 Pa could not be reached with these and other PEO-SAs, even with the addition of up to 17.3 wt% added HMDS-treated silica filler. A non-amphiphilic PEO-silane control, despite higher PEO wt% (2.99 wt%) versus all PEO-SAs, achieved neither surface-restructuring nor did it produce a measurable yield stress. Instead, Sylgard 184 was modified with Star [SP] and Triblock [SP] as well as 17.3 wt% of DiMeDi-treated silica filler. Each of these formulations exceeded the targeted yield stress [Star [SP] (1,405 Pa) and Triblock [SP] (3,385 Pa)]. These formulations also surpassed the targeted recovered G' (>1000 Pa) and were well below the necessary loss factor (<0.8): [Star [SP] (11,023 Pa; 0.56) and Triblock [SP] (8286 Pa; 0.63)]. In addition to the notable thixotropic properties of the Triblock [SP]-modified silicone, extensive water-driven restructuring was observed ($\theta_{static,\ 5\ min}$ 44°). Thus, the unique properties of the Star [SP] and Triblock [SP] PEO-SAs may result from their combination of PEO-content, architecture and non-crosslinkability. The utility of these PEO-SAs to produce thixotropic Sylgard 184 with optional water-driven surface hydrophilicity should advance the fabrication of 3D printed objects in a variety of applications.

Conflicts of interest

There are no conflicts to declare.

Acknowledgements

This work was supported by the U.S. Department of Energy through the Los Alamos National Laboratory Enhanced Surveillance Program. Los Alamos National Laboratory is operated by Los Alamos National Security, LLC, for the National Nuclear Security Administration of U.S. Department of Energy (Contract DEAC52-06NA25396). The authors also thank the Texas A&M Engineering and Experiment Station (TEES).

References

1. Ratner, B. D.; Hoffman, A. S.; Schoen, F. J.; Lemons, J. E., *Biomaterials science: An introduction to materials in medicine*. Elsevier Academic Press: 2004; p 697-707.
2. El-Zaim, H. S.; Heggers, J. P., In *Polymeric Biomaterials*, 2nd ed.; Marcel Dekker, Inc.: New York, NY, 2002.
3. Feldman, K.; Hähner, G.; Spencer, N. D.; Harder, P.; Grunze, M., Probing resistance to protein adsorption of oligo(ethylene glycol)-terminated self-assembled monolayers by scanning force microscopy. *J. Am. Chem. Soc.* **1999**, 10134-10141.
4. Aziz, T.; Waters, M.; Jagger, R., Development of a new poly(dimethylsiloxane) maxillofacial prosthetic material. *J. Biomed. Mater. Res. B Appl. Biomater.* **2003**, 252-261.
5. Guo, X.; Huang, Y.; Cai, X.; Liu, C.; Liu, P. J. M. S.; Technology, Capacitive wearable tactile sensor based on smart textile substrate with carbon black/silicone rubber composite dielectric. *Meas. Sci. Technol.* **2016**, 045105.
6. Kim, T. A.; Kim, H. S.; Lee, S. S.; Park, M., Single-walled carbon nanotube/silicone rubber composites for compliant electrodes. *Carbon* **2012**, 444-449.
7. Xu, S.; Zhang, Y.; Cho, J.; Lee, J.; Huang, X.; Jia, L.; Fan, J. A.; Su, Y.; Su, J.; Zhang, H.; Cheng, H.; Lu, B.; Yu, C.; Chuang, C.; Kim, T.-i.; Song, T.; Shigeta, K.; Kang, S.; Dagdeviren, C.; Petrov, I.; Braun, P. V.; Huang, Y.; Paik, U.; Rogers, J. A., Stretchable batteries with self-similar serpentine interconnects and integrated wireless recharging systems. *Nat. Commun.* **2013**, 1543.
8. Coyle, S.; Majidi, C.; LeDuc, P.; Hsia, K. J., Bio-inspired soft robotics: Material selection, actuation, and design. *Extreme Mech. Lett.* **2018**, 51-59.
9. Zhalmuratova, D.; Chung, H.-J., Reinforced gels and elastomers for biomedical and soft robotics applications. *ACS Appl. Polym. Mater.* **2020**, 1073-1091.
10. Gomes, R. N.; Borges, I.; Pereira, A. T.; Maia, A. F.; Pestana, M.; Magalhães, F. D.; Pinto, A. M.; Gonçalves, I. C., Antimicrobial graphene nanoplatelets coatings for silicone catheters. *Carbon* **2018**, 635-647.
11. Li, M.; Neoh, K. G.; Xu, L. Q.; Wang, R.; Kang, E.-T.; Lau, T.; Olszyna, D. P.; Chiong, E., Surface modification of silicone for biomedical applications requiring long-term antibacterial, antifouling, and hemocompatible properties. *Langmuir* **2012**, 16408-16422.
12. Mitra, A.; Choudhary, S.; Garg, H.; H G, J., Maxillofacial prosthetic materials- an inclination towards silicones. *J. Clin. Diagnostic Res.* **2014**, ZE08-ZE13.
13. Wu, A. S.; Small Iv, W.; Bryson, T. M.; Cheng, E.; Metz, T. R.; Schulze, S. E.; Duoss, E. B.; Wilson, T. S., 3D printed silicones with shape memory. *Sci. Rep.* **2017**, 4664.
14. Unkovskiy, A.; Spintzyk, S.; Brom, J.; Huettig, F.; Keutel, C., Direct 3D printing of silicone facial prostheses: A preliminary experience in digital workflow. *J. Prosthet. Dent.* **2018**, 303-308.
15. Jungst, T.; Smolan, W.; Schacht, K.; Scheibel, T.; Groll, J., Strategies and molecular design criteria for 3D printable hydrogels. *Chem. Rev.* **2016**, 1496-1539.
16. Bibars, A. R. M.; Al-Hourani, Z.; Khader, Y.; Waters, M., Effect of thixotropic agents as additives on the mechanical properties of maxillofacial silicone elastomers. *J. Prosthet. Dent.* **2018**, 671-675.
17. Lewis, J. A., Direct ink writing of 3D functional materials. *Adv. Funct. Mater.* **2006**, 2193-2204.
18. Duoss, E. B.; Weisgraber, T. H.; Hearon, K.; Zhu, C.; Small Iv, W.; Metz, T. R.; Vericella, J. J.; Barth, H. D.; Kuntz, J. D.; Maxwell, R. S.; Spadaccini, C. M.; Wilson, T. S., Three-dimensional printing of elastomeric, cellular architectures with negative stiffness. *Adv. Funct. Mater.* **2014**, 4905-4913.
19. Lepowsky, E.; Tasoglu, S., Emerging anti-fouling methods: towards reusability of 3D-printed devices for biomedical applications. *Micromachines* **2018**, 196.
20. Wolf, M. P.; Salieb-Beugelaar, G. B.; Hunziker, P., PDMS with designer functionalities—Properties, modifications strategies, and applications. *Prog. Polym. Sci.* **2018**, 97-134.
21. Efimenko, K.; Wallace, W. E.; Genzer, J., Surface modification of Sylgard-184 poly(dimethyl siloxane) networks by ultraviolet and ultraviolet/ozone treatment. *J. Colloid Interface Sci.* **2002**, 306-315.
22. Lin, D.; Zhao, Q.; Yan, M., Surface modification of polydimethylsiloxane microfluidic chips by polyamidoamine dendrimers for amino acid separation. *J. Appl. Polym. Sci.* **2016**.
23. Béfahy, S.; Lipnik, P.; Pardoen, T.; Nascimento, C.; Patris, B.; Bertrand, P.; Yunus, S., Thickness and elastic modulus of plasma treated PDMS silica-like surface layer. *Langmuir* **2010**, 3372-3375.
24. de Campos, R. P. S.; Yoshida, I. V. P.; da Silva, J. A. F., Surface modification of PDMS microchips with poly(ethylene glycol) derivatives for μTAS applications. *Electrophoresis* **2014**, 2346-2352.
25. Murthy, R.; Cox, C. D.; Hahn, M. S.; Grunlan, M. A., Protein-resistant silicones: Incorporation of poly(ethylene oxide) via siloxane tethers. *Biomacromolecules* **2007**, 3244-3252.

26. Hawkins, M. L.; Grunlan, M. A., The protein resistance of silicones prepared with a PEO-silane amphiphile. *J. Mater. Chem.* **2012**, 19540-19546.
27. Hawkins, M. L.; Rufin, M. A.; Raymond, J. E.; Grunlan, M. A., Direct observation of the nanocomplex surface reorganization of antifouling silicones containing a highly mobile PEO-silane amphiphile. *J. Mater. Chem. B* **2014**, 5689-5697.
28. Rufin, M. A.; Gruetzner, J. A.; Hurley, M. J.; Hawkins, M. L.; Raymond, E. S.; Raymond, J. E.; Grunlan, M. A., Enhancing the protein resistance of silicone via surface-restructuring PEO–silane amphiphiles with variable PEO length. *J. Mater. Chem. B* **2015**, 2816-2825.
29. Rufin, M. A.; Barry, M. E.; Adair, P. A.; Hawkins, M. L.; Raymond, J. E.; Grunlan, M. A., Protein resistance efficacy of PEO-silane amphiphiles: Dependence on PEO-segment length and concentration. *Acta Biomater.* **2016**, 247-252.
30. Rufin, M. A.; Ngo, B. K. D.; Barry, M. E.; Page, V. M.; Hawkins, M. L.; Stafslien, S. J.; Grunlan, M. A., Antifouling silicones based on surface-modifying additive amphiphiles. *Green Mater.* **2017**, 4-13.
31. Hawkins, M. L.; Schott, S. S.; Grigoryan, B.; Rufin, M. A.; Ngo, B. K. D.; Vanderwal, L.; Stafslien, S. J.; Grunlan, M. A., Anti-protein and anti-bacterial behavior of amphiphilic silicones. *Polym. Chem.* **2017**, 5239-5251.
32. Ngo, B. K. D.; Lim, K. K.; Stafslien, S. J.; Grunlan, M. A., Stability of silicones modified with PEO-silane amphiphiles: Impact of structure and concentration. *Polym. Degradation Stab.* **2019**, 136-142.
33. Ngo, B. K. D.; Barry, M. E.; Lim, K. K.; Johnson, J. C.; Luna, D. J.; Pandian, N. K. R.; Jain, A.; Grunlan, M. A., Thromboresistance of silicones modified with PEO-silane amphiphiles. *ACS Biomater. Sci. Eng.* **2020**, 2029-2037.
34. Dogbevi, K. S.; Ngo, B. K. D.; Blake, C. W.; Grunlan, M. A.; Coté, G. L., Pumpless, "self-driven" microfluidic channels with controlled blood flow using an amphiphilic silicone. *ACS Appl. Polym. Mater.* **2020**, 1731-1738.
35. Jindal, S. K.; Sherriff, M.; Waters, M. G.; Smay, J. E.; Coward, T. J., Development of a 3D printable maxillofacial silicone: Part II. optimization of moderator and thixotropic agent. *J. Prosthet. Dent.* **2018**, 299-304.
36. Ozbolat, V.; Dey, M.; Ayan, B.; Povilianskas, A.; Demirel, M. C.; Ozbolat, I. T., 3D printing of PDMS improves its mechanical and cell adhesion properties. *ACS Biomater. Sci. Eng.* **2018**, 682-693.
37. Hinton, T. J.; Hudson, A.; Pusch, K.; Lee, A.; Feinberg, A. W., 3D printing PDMS elastomer in a hydrophilic support bath via freeform reversible embedding. *ACS Biomater. Sci. Eng.* **2016**, 1781-1786.
38. Nguyen, K. D. Q.; Megone, W. V.; Kong, D.; Gautrot, J. E., Ultrafast diffusion-controlled thiol–ene based crosslinking of silicone elastomers with tailored mechanical properties for biomedical applications. *Polym. Chem.* **2016**, 5281-5293.
39. Xu, X.; Gao, C.; Zheng, Q., Rheological characterization of room temperature vulcanized silicone sealant: Effect of filler particle size. *Polym. Eng. Sci.* **2008**, 656-661.
40. Romasanta, L. J.; Lopez-Manchado, M. A.; Verdejo, R., The role of carbon nanotubes in both physical and chemical liquid–solid transition of polydimethylsiloxane. *Eur. Polym. J.* **2013**, 1373-1380.
41. Yue, Y.; Zhang, C.; Zhang, H.; Zhang, D.; Chen, X.; Chen, Y.; Zhang, Z., Rheological behaviors of fumed silica filled polydimethylsiloxane suspensions. *Compos. Part A Appl. Sci. Manuf.* **2013**, 152-159.
42. Courtial, E.-J.; Perrinet, C.; Colly, A.; Mariot, D.; Frances, J.-M.; Fulchiron, R.; Marquette, C., Silicone rheological behavior modification for 3D printing: Evaluation of yield stress impact on printed object properties. *Addit. Manuf.* **2019**, 50-57.
43. Li, L.; Lin, Q.; Tang, M.; Duncan, A. J. E.; Ke, C., Advanced polymer designs for direct-ink-write 3D printing. *Chem. Eur. J.* **2019**, 10768-10781.